

# Optimal Voltage Phasor Regulation for Switching Actions in Unbalanced Distribution Systems

Michael D. Sankur\*, Roel Dobbe†, Alexandra von Meier‡, Emma M. Stewart§, Daniel B. Arnold\*

\*Lawrence Berkeley National Lab, Berkeley, CA USA, †AI Now Institute, New York, NY USA

‡University of California, Berkeley, Berkeley, CA USA, §Lawrence Livermore National Lab, Livermore, CA USA  
msankur@lbl.gov, roel@ainowinstitute.org, vonmeier@berkeley.edu, stewart78@llnl.gov, dbarnold@lbl.gov

**Abstract**—Proliferation of Distributed Energy Resources (DERs) and Phasor Measurement Units (PMUs) into electric power distribution grids presents new opportunities for utility operators to manage distribution systems more effectively. In this work we formulate an Optimal Power Flow (OPF) approach that manages DER power injections to minimize the voltage phasor difference between two nodes on a distribution network with the goal of enabling efficient network reconfiguration. To accomplish this, we develop a linear model that relates voltage phase angles to active and reactive power flows in unbalanced distribution systems. Used in conjunction with existing linearizations relating voltage magnitudes to power flows, we formulate an OPF capable of minimizing the voltage phasor difference between two points in a network. In simulations, we explore the use of the developed approach to minimize the phasor difference across switches to be closed, thereby providing an opportunity to automate and increase the speed of reconfiguration in unbalanced distribution grids.

**Index Terms**—Voltage phasor regulation, Optimal power flow, Distributed energy resources

## I. INTRODUCTION

The Proliferation of phasor measurement units (PMUs) into electric power distribution system is providing deeper insights into grid operation, and may serve to better inform the process of managing distributed energy resources (DERs). Distribution PMUs provide time-stamped measurements of magnitude and angle of voltage and current phasors. These devices are increasingly ubiquitous as standalone units [1], or are being incorporated into other system components [2]. There is a a small, but growing, number of control applications [3], [4] that use phase angle measurements, indicating that sufficient PMU infrastructure may be in place in future distribution grids to support control activities with decisions based on feeder voltage phasor measurements.

The ability to reconfigure distribution feeders and island/reconnect microgrids are two important applications of future grids [5], [6]. Distribution PMU data and DER management may be important tools for enabling fast and safe switching of circuit elements for the goal of network reconfiguration. To close a switch, the voltage magnitude difference and voltage angle difference between both sides should be sufficiently small to prevent arcing and transient currents. As such, to

This work was supported in part by the U.S. Department of Energy ARPA-E program (DE-AR0000340), and the Department of Energy Office of Energy Efficiency and Renewable Energy under Contract No. DE-AC02-05CH11231.

facilitate network reconfiguration, distribution system operators (DSOs) typically employ backup power injection at strategic reconfiguration locations to minimize voltage phasor difference across switches. In the case where a reconfiguration is planned, DSOs may schedule such actions in advance, and send mobile generators with back up power to the correct locations. After an unplanned power outage, it may take considerable time to deploy engineering staff with backup power to necessary switching locations.

DERs present an opportunity to facilitate network reconfiguration at timescales much faster than with current practices. With sufficient amount and proper location of DERs, it may be possible to control the voltage phasor at strategic points in the network, alleviating the need for ad-hoc deployment of generation assets for switching.

There is sparse literature on strategies that aim to *directly control the voltage phasor in unbalanced systems in an optimal power flow (OPF) formulation*. Due to the nonlinear nature of power flow, many OPFs are formulated as quadratically constrained quadratic programs (QCQPs). A popular method for analyzing such OPFs is relaxation via semidefinite programming (SDP) [7]. It is well documented that relaxation of OPF problems via SDP often fails to achieve a rank-one solution [7], [8], [9] for complex networks, or without altering the original optimization program. Our first efforts in the area of controlling voltage phasors employed SDP relaxations of QCQPs. In these efforts, we found little success in obtaining a rank-one solution when testing with non-simple radial networks or meshed networks [10].

The difficulties of OPFs formulated as QCQPs and analyzed as SDPs limit the applicability and practicality of these approaches. Therefore, we are motivated to create a linear approximation for power flow that sufficiently captures the mapping between the entire voltage phasor and power, is sufficiently accurate for control purposes, and can be incorporated into convex OPF formulations.

To enable a control strategy that can regulate voltage phasors, in this work we extend a linearized model of three phase power flow to include a mapping of voltage phase angle differences into network active and reactive power flows. To our knowledge, OPF approaches controlling voltage magnitude, active and reactive power flows, but not voltage angle, cannot always effectively minimize voltage phasor difference across an open switch. This motivates the extension of the linear mappings which relate voltage magnitude to active and

## NOMENCLATURE

$\mathcal{P}_n$	Set of phases that exist at node $n$
$\mathcal{P}_{mn}$	Set of phases that exist on line $(m, n)$
$V_n^\phi$	Voltage phasor on phase $\phi$ at node $n$
$E_n^\phi$	Squared magnitude of voltage on phase $\phi$ at node $n$
$\theta_n^\phi$	Angle of voltage phasor on phase $\phi$ at node $n$
$Z_{mn}^{\phi\psi}$	Impedance of line $(m, n)$ between phases $(\phi, \psi)$
$I_{mn}^\phi$	Current phasor on phase $\phi$ on line $(m, n)$
$S_{mn}^\phi$	Phasor of complex power entering node $n$ on phase $\phi$ on line $(m, n)$
$s_n^\phi$	Complex nodal power phasor on phase $\phi$ at node $n$
$w_n^\phi$	Controllable complex power dispatch on phase $\phi$ at node $n$
$(\cdot)^*$	Complex conjugate

reactive power flows [11], [12], [13], to consider the entire voltage phasor. Our contribution is an extension of these results to include a linear relation between complex line power flow and voltage angle difference, in Section II-C.

The specific activity studied herein is an OPF formulation that minimizes the voltage phasor difference across an open switch in a distribution system while simultaneously regulating feeder voltage magnitudes to within acceptable limits. In driving the voltage phasor difference across a circuit element to 0, we ensure that when the switch is closed only small amounts of power will flow across this element reducing the risk of arcing and instantaneous power flow surges.

The paper is organized as follows: A derivation of a linearized model of unbalanced power flow that maps voltage phasor differences into active and reactive power flows is presented in Section II. Simulation results of an OPF that incorporates the linearized power flow model to minimize voltage phasor differences across a line are presented in Section III. Concluding remarks are provided in Section IV.

## II. ANALYSIS

In this section, we derive the linearized mapping between voltage angle and power flow. Please refer to the nomenclature table for variable definitions.

## A. Preliminaries

Let  $\mathcal{T} = (\mathcal{N}, \mathcal{L})$  denote a graph representing an unbalanced distribution feeder, where  $\mathcal{N}$  is the set of nodes of the feeder and  $\mathcal{L}$  is the set of line segments. Nodes are indexed by  $m$  and  $n$ , with  $m, n \in \mathcal{N}$ . Let  $\mathcal{N} \triangleq \{\infty, 0, 1, \dots, |\mathcal{N}|\}$ , where node 0 denotes the substation (feeder head). Immediately upstream of node 0 is an additional node used to represent the transmission system, indexed by  $\infty$ . We treat node  $\infty$  as an infinite bus, decoupling interactions in the downstream distribution system from the rest of the grid. While the substation voltage may evolve over time, we assume this evolution takes place independently of DER control actions in  $\mathcal{T}$ . Lines are indexed by  $(m, n)$ , with line  $(m, n)$  connecting nodes  $m$  and  $n$ .

Each node and line segment in  $\mathcal{T}$  can have up to three phases, labeled  $a$ ,  $b$ , and  $c$ . Phases are referred to by  $\phi \in \{a, b, c\}$  and  $\psi \in \{a, b, c\}$ . We define  $\mathcal{P}_m$  and  $\mathcal{P}_n$  as the set of phases at nodes  $m$  and  $n$ , respectively, and  $\mathcal{P}_{mn}$  as set of phases of line segment  $(m, n)$ . If phase  $\phi$  is present at node  $m$ , then at least one line connected to  $m$  must contain phase

$\phi$ . If line  $(m, n)$  exists, its phases are a subset of the phases present at both node  $m$  and node  $n$ , such that  $(m, n) \in \mathcal{L} \Rightarrow \mathcal{P}_{mn} \subseteq \mathcal{P}_m \cap \mathcal{P}_n$ .

The current/voltage relationship for a three phase line  $(m, n)$  between adjacent nodes  $m$  and  $n$  is captured by Kirchhoff's Voltage Law (KVL) in full and vector form (1), indexed by  $\mathcal{P}_{mn}$ :

$$\begin{bmatrix} V_m^a \\ V_m^b \\ V_m^c \end{bmatrix} = \begin{bmatrix} V_n^a \\ V_n^b \\ V_n^c \end{bmatrix} + \begin{bmatrix} Z_{mn}^{aa} & Z_{mn}^{ab} & Z_{mn}^{ac} \\ Z_{mn}^{ba} & Z_{mn}^{bb} & Z_{mn}^{bc} \\ Z_{mn}^{ca} & Z_{mn}^{cb} & Z_{mn}^{cc} \end{bmatrix} \begin{bmatrix} I_{mn}^a \\ I_{mn}^b \\ I_{mn}^c \end{bmatrix}_{\mathcal{P}_{mn}}, \\ [V_m = V_n + Z_{mn} I_{mn}]_{\mathcal{P}_{mn}}. \quad (1)$$

where,  $Z_{mn}^{\phi\psi} = r_{mn}^{\phi\psi} + jx_{mn}^{\phi\psi}$  is the complex impedance of line  $(m, n)$  across phases  $\phi$  and  $\psi$ ,  $V_m = [V_m^a, V_m^b, V_m^c]^T$ , and  $I_{mn} = [I_{mn}^a, I_{mn}^b, I_{mn}^c]^T$ .

To index (1) by the set of line phases  $\mathcal{P}_{mn}$  the rows associated with phases  $\psi \notin \mathcal{P}_{mn}$  of (1) are removed, as are the appropriate columns  $Z_{mn}$  and other matrices. To give two examples, if  $\mathcal{P}_{mn} = \{a\}$ , then (1) is  $[V_m]_{\{a\}} \equiv V_m^a = V_n^a + Z_{mn}^{aa} I_{mn}^a$ , and if  $\mathcal{P}_{mn} = \{a, c\}$  then (1) is:

$$[V_m]_{\{a, c\}} \equiv \begin{bmatrix} V_m^a \\ V_m^c \end{bmatrix} = \begin{bmatrix} V_n^a \\ V_n^c \end{bmatrix} + \begin{bmatrix} Z_{mn}^{aa} & Z_{mn}^{ac} \\ Z_{mn}^{ca} & Z_{mn}^{cc} \end{bmatrix} \begin{bmatrix} I_{mn}^a \\ I_{mn}^c \end{bmatrix}.$$

The reader should note that if  $\phi \notin \mathcal{P}_n$  (phase  $\phi$  does not exist at node  $n$ ), then all variables associated with phase  $\phi$  at node  $n$  are 0. If  $\phi \notin \mathcal{P}_{mn}$  (i.e. phase  $\phi$  does not exist on line segment  $(m, n)$ ), then all variables associated with phase  $\phi$  on line  $(m, n)$  are 0.

Throughout this work, we use the symbol  $\circ$  to represent the Hadamard product of two matrices of the same dimension, also known as the element-wise product, and the symbol  $\oslash$  to represent Hadamard division between two matrices of the same dimension.

## B. Complex Power

In our model, a voltage dependent complex load  $s_n^\phi$  is served on all existing phases at each node except the substation and node representing the transmission line, defined as:

$$s_n^\phi (V_n^\phi) = (\beta_{S,n}^\phi + \beta_{Z,n}^\phi E_n^\phi) d_n^\phi + w_n^\phi - jc_n^\phi, \quad (2)$$

where  $d_n^\phi$  is the complex demand, with constant power coefficient  $\beta_{S,n}^\phi$  and constant impedance coefficient  $\beta_{Z,n}^\phi$ , with  $\beta_{S,n}^\phi + \beta_{Z,n}^\phi = 1$ ,  $w_n^\phi = u_n^\phi + jv_n^\phi$  is the complex power available for control (e.g. DER),  $c_n^\phi$  denotes capacitance, and  $E_n^\phi = |V_n^\phi|^2$  is the squared voltage magnitude, all for  $\phi \in \mathcal{P}_n$ .

We use the common definition of complex power on phase  $\phi$  of line  $(m, n)$  as  $S_{mn}^\phi = V_n^\phi (I_{mn}^\phi)^*$ . The vector of complex power phasors at node  $n$  for line  $(m, n)$  is  $S_{mn} = V_n \circ I_{mn}^*$ . Complex power balance at a node  $m$  is given by (3):

$$\sum_{l:(l,m) \in \mathcal{L}} S_{lm} = s_m + \sum_{n:(m,n) \in \mathcal{L}} S_{mn} + L_{mn}, \quad (3)$$

where  $S_{mn} = [S_{mn}^a, S_{mn}^b, S_{mn}^c]^T$ ,  $s_m = [s_m^a, s_m^b, s_m^c]^T$  is the vector of complex loads at node  $m$ , and  $S_{mn}^\phi = 0, \forall \phi \notin \mathcal{P}_{mn}$ .

$\mathcal{P}_{mn}$  and  $s_m^\phi = 0, \forall \phi \notin \mathcal{P}_m$ . Following the analysis in [11] and [12], we assume the loss term  $\mathbf{L}_{mn}$  in (3) is negligible such that  $\mathbf{L}_{mn} = [0, 0, 0]^T, \forall (m, n) \in \mathcal{L}$ .

### C. Voltage Angle

We now derive a mapping between line power flow and voltage phasor angle difference on an unbalanced line. We begin by computing the Hadamard product of the complex conjugate (non-transposed) of (1) and the vector of voltage phasors at node  $n$ ,  $\mathbf{V}_n$ :

$$[\mathbf{V}_m^* \circ \mathbf{V}_n = \mathbf{V}_n^* \circ \mathbf{V}_n + \mathbf{Z}_{mn}^* \mathbf{I}_{mn}^* \circ \mathbf{V}_n]_{\mathcal{P}_{mn}}. \quad (4)$$

We then substitute for the current vector  $\mathbf{I}_{mn}$  using the definition of power,  $\mathbf{I}_{mn}^* = \mathbf{S}_{mn} \oslash \mathbf{V}_{mn}$ :

$$[\mathbf{V}_m^* \circ \mathbf{V}_n = \mathbf{V}_n^* \circ \mathbf{V}_n + \mathbf{Z}_{mn}^* (\mathbf{S}_{mn} \oslash \mathbf{V}_n) \circ \mathbf{V}_n]_{\mathcal{P}_{mn}}. \quad (5)$$

Applying the analysis in [11], [12], we approximate voltages as balanced, and rearrange terms on the RHS, giving:

$$[\mathbf{V}_m^* \circ \mathbf{V}_n = \mathbf{V}_n^* \circ \mathbf{V}_n + (\mathbf{A} \circ \mathbf{Z}_{mn}^*) \mathbf{S}_{mn}]_{\mathcal{P}_{mn}}, \quad (6)$$

where:

$$\mathbf{A} = \begin{bmatrix} 1 & \alpha & \alpha^2 \\ \alpha^2 & 1 & \alpha \\ \alpha & \alpha^2 & 1 \end{bmatrix}, \quad (7)$$

$$\alpha = 1 \exp(j2\pi/3) = 1\angle 120^\circ = \frac{1}{2}(-1 + j\sqrt{3}). \quad (8)$$

We now look at the LHS of (6), and recognize that the elements of  $\mathbf{V}_m^* \circ \mathbf{V}_n$  are  $|V_m^\phi| |V_n^\phi| (\cos(\theta_n^\phi - \theta_m^\phi) + j \sin(\theta_n^\phi - \theta_m^\phi)), \phi \in \mathcal{P}_{mn}$ . We therefore take the imaginary component of (6):

$$\left[ \begin{bmatrix} |V_m^a| |V_n^a| \sin(\theta_n^a - \theta_m^a) \\ |V_m^b| |V_n^b| \sin(\theta_n^b - \theta_m^b) \\ |V_m^c| |V_n^c| \sin(\theta_n^c - \theta_m^c) \end{bmatrix} = \mathbf{Im}\{(\mathbf{A} \circ \mathbf{Z}_{mn}^*) \mathbf{S}_{mn}\} \right]_{\mathcal{P}_{mn}}. \quad (9)$$

To simplify (9), we introduce two assumptions. First, we assume that the small angle approximation holds, such that  $\sin(\theta_m^\phi - \theta_n^\phi) \approx \theta_m^\phi - \theta_n^\phi, \forall \phi \in \mathcal{P}_{mn}, \forall (m, n) \in \mathcal{L}$ . Second, we assume that  $|V_m^\phi| |V_n^\phi| \approx 1, \forall \phi \in \mathcal{P}_{mn}, \forall (m, n) \in \mathcal{L}$ . Applying these two assumptions and negating (9) gives:

$$[\boldsymbol{\theta}_m - \boldsymbol{\theta}_n \approx -\mathbf{Im}\{(\mathbf{A} \circ \mathbf{Z}_{mn}^*) \mathbf{S}_{mn}\}]_{\mathcal{P}_{mn}}, \quad (10)$$

where  $\boldsymbol{\theta}_m = [\theta_m^a, \theta_m^b, \theta_m^c]^T$  is the vector of voltage phasor angles at node  $m$ . Finally, we apply the **Im** operator on the RHS, and obtain:

$$[\boldsymbol{\theta}_m \approx \boldsymbol{\theta}_n - \mathbf{N}_{mn} \mathbf{P}_{mn} - \mathbf{M}_{mn} \mathbf{Q}_{mn}]_{\mathcal{P}_{mn}}, \quad (11)$$

$$[\mathbf{M}_{mn} = \mathbf{Re}\{\mathbf{A} \circ \mathbf{Z}_{mn}^*\}]_{\mathcal{P}_{mn}}, \quad (12)$$

$$[\mathbf{N}_{mn} = \mathbf{Im}\{\mathbf{A} \circ \mathbf{Z}_{mn}^*\}]_{\mathcal{P}_{mn}}, \quad (13)$$

where  $\mathbf{P}_{mn} = [P_{mn}^a, P_{mn}^b, P_{mn}^c]^T$  is the vector of active powers on line  $(m, n)$ ,  $\mathbf{Q}_{mn} = [Q_{mn}^a, Q_{mn}^b, Q_{mn}^c]^T$  is the vector of reactive powers on line  $(m, n)$ ,  $S_{mn}^\phi = P_{mn}^\phi + jQ_{mn}^\phi$ , and  $\mathbf{S}_{mn} = \mathbf{P}_{mn} + j\mathbf{Q}_{mn}$ .

We arrive at a linear mapping between voltage phasor angle difference and line complex power flow on line

$(m, n)$ . The matrices  $\mathbf{M}_{mn}$  and  $\mathbf{N}_{mn}$  are modified impedance matrices, where the off-diagonal elements are rotated by  $\pm 120^\circ$  (see (7)). The diagonal entries of  $\mathbf{M}_{mn}$  are  $r_{mn}^{\phi\phi}$ . Off-diagonal entries of  $\mathbf{M}_{mn}$  are  $\frac{1}{2}(-r_{mn}^{\phi\psi} + \sqrt{3}x_{mn}^{\phi\psi})$  for  $(\phi, \psi) \in \{ab, bc, ca\}$ , and  $\frac{1}{2}(-r_{mn}^{\phi\psi} - \sqrt{3}x_{mn}^{\phi\psi})$  for  $(\phi, \psi) \in \{ac, ba, cb\}$ . The diagonal entries of  $\mathbf{N}_{mn}$  are  $-x_{mn}^{\phi\phi}$ . Off-diagonal entries of  $\mathbf{N}_{mn}$  are  $\frac{1}{2}(x_{mn}^{\phi\psi} + \sqrt{3}r_{mn}^{\phi\psi})$  for  $(\phi, \psi) \in \{ab, bc, ca\}$ , and  $\frac{1}{2}(x_{mn}^{\phi\psi} - \sqrt{3}r_{mn}^{\phi\psi})$  for  $(\phi, \psi) \in \{ac, ba, cb\}$ .

### D. Voltage Magnitude

The mapping between squared voltage magnitude and complex power flow on a line is derived in [11] and [12]. For completeness, we present this mapping in our notation:

$$[\mathbf{E}_m \approx \mathbf{E}_n + 2\mathbf{M}_{mn} \mathbf{P}_{mn} - 2\mathbf{N}_{mn} \mathbf{Q}_{mn}]_{\mathcal{P}_{mn}}, \quad (14)$$

where  $\mathbf{E}_m = [E_m^a, E_m^b, E_m^c]^T$  is a vector of squared voltage magnitudes at node  $m$ .

### E. Linearized Unbalanced Power Flow Model

We now present the full set of equations that comprise a linearized model for unbalanced power flow.

Per phase node complex load

$$\forall \phi \in \mathcal{P}_m, \forall m \in \mathcal{N} \setminus \{\infty, 0\}$$

$$s_m^\phi (E_m^\phi) = (\beta_{S,m}^\phi + \beta_{Z,m}^\phi E_m^\phi) d_m^\phi + w_m^\phi - j c_m^\phi \quad (15)$$

Node complex power balance

$$\forall m \in \mathcal{N}$$

$$\sum_{l:(l,m) \in \mathcal{L}} \mathbf{S}_{lm} \approx \mathbf{s}_m + \sum_{n:(m,n) \in \mathcal{L}} \mathbf{S}_{mn} \quad (16)$$

Magnitude and angle equations for lines

$$\forall (m, n) \in \mathcal{L}$$

$$[\mathbf{E}_m \approx \mathbf{E}_n + 2\mathbf{M}_{mn} \mathbf{P}_{mn} - 2\mathbf{N}_{mn} \mathbf{Q}_{mn}]_{\mathcal{P}_{mn}} \quad (17)$$

$$[\boldsymbol{\theta}_m \approx \boldsymbol{\theta}_n - \mathbf{N}_{mn} \mathbf{P}_{mn} - \mathbf{M}_{mn} \mathbf{Q}_{mn}]_{\mathcal{P}_{mn}} \quad (18)$$

$$[\mathbf{M}_{mn} = \mathbf{Re}\{\mathbf{A} \circ \mathbf{Z}_{mn}^*\}]_{\mathcal{P}_{mn}} \quad (19)$$

$$[\mathbf{N}_{mn} = \mathbf{Im}\{\mathbf{A} \circ \mathbf{Z}_{mn}^*\}]_{\mathcal{P}_{mn}} \quad (20)$$

$$\mathbf{A} = \begin{bmatrix} 1 & \alpha & \alpha^2 \\ \alpha^2 & 1 & \alpha \\ \alpha & \alpha^2 & 1 \end{bmatrix} \quad (21)$$

$$\alpha = 1 \exp(j2\pi/3) = 1\angle 120^\circ = \frac{1}{2}(-1 + j\sqrt{3}) \quad (22)$$

### III. PHASOR TRACKING FOR SWITCHING OPERATIONS

We now present an experiment in which the complete linearized unbalanced power flow model, (15) – (21), is incorporated into an OPF with the objective of minimizing the phasor difference between nodes at the ends of one or more open switches (we will refer to this as phasor tracking), while regulating system voltage magnitudes to within acceptable limits. The OPF decision variables were DER active and reactive power injections at select nodes, and were capacity constrained.

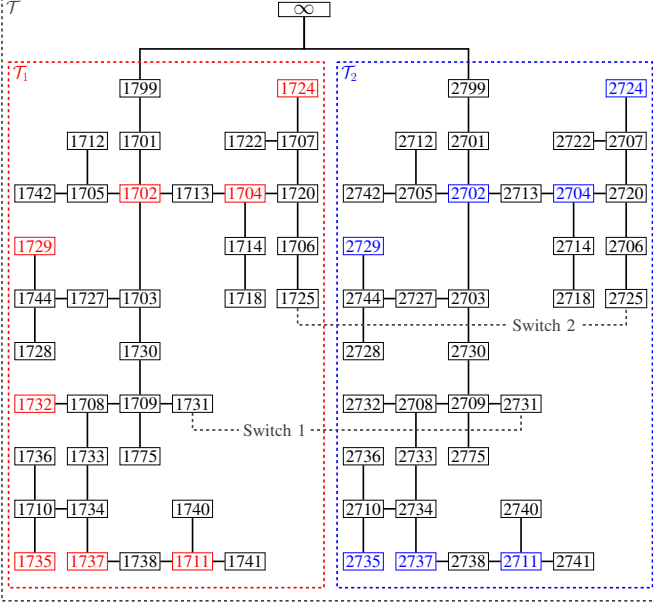


**Fig. 1:** Networks  $\mathcal{T}_1$  and  $\mathcal{T}_2$  connected to the same transmission line, with two open switches between them. Nodes with DER resources are highlighted in red for  $\mathcal{T}_1$  and blue for  $\mathcal{T}_2$ .

The scenario we discuss is the reconfiguration of distribution networks through switching actions. We do not consider economic activity or optimization in these experiments, rather we assume that DER dispatch for economic purposes is suspended in order to devote said resources to reconfiguration efforts.

Our experiment considered two switching actions that each add a link between two distribution networks. Networks  $\mathcal{T}_1$  and  $\mathcal{T}_2$ , are connected to the same transmission line as shown in Fig. 1. The overall network is  $\mathcal{T} = (\mathcal{N}, \mathcal{E})$  with  $\mathcal{N} = \mathcal{N}_1 \cup \mathcal{N}_2 \cup \infty$  and  $\mathcal{E} = \mathcal{E}_1 \cup \mathcal{E}_2 \cup (\infty, 1799) \cup (\infty, 2799)$ . Both  $\mathcal{T}_1$  and  $\mathcal{T}_2$  were modified versions of the IEEE 37 node test feeder model. Feeder topology, line configuration, line impedance, line length, and spot loads are specified in [14]. For clarity, we add the number 1 to the front of nodes within  $\mathcal{N}_1$  and the number 2 for nodes within  $\mathcal{N}_2$  (e.g. node 799 of  $\mathcal{N}_1$  is now 1799 and node 775 of  $\mathcal{N}_2$  is now 2775). The transmission line was treated as an infinite bus, with a fixed voltage reference of  $\mathbf{V}_\infty = [1, 1\angle 240^\circ, 1\angle 120^\circ]^T$  p.u. The transmission line is connected to node 1799 of  $\mathcal{N}_1$  (node 799 in [14]) and 2799 of  $\mathcal{N}_2$  (node 799 in [14]).

The voltage regulators between nodes 1799 and 1701, and between nodes 2799 and 2701, were both omitted. The transformers between nodes 1709 and 1775, and between 1709 and 1775, were both replaced by a line of configuration 724 (according to [14], page 5) and length of 50 feet. All loads were assumed to be Wye connected on the phase specified in [14]. For both networks, the voltage dependent load model of (2) had parameters  $\beta_{S,n}^\phi = 0.85$  and  $\beta_{Z,n}^\phi = 0.15 \forall \phi \in \mathcal{P}_n, \forall n \in \mathcal{N}$ . To create a load imbalance between the two networks, we multiplied all loads in  $\mathcal{T}_1$  by a factor of 1.5, and all loads in  $\mathcal{T}_2$  by a factor of 1.75.

An open switch was placed between node 1731 of  $\mathcal{N}_1$  and node 2731 of  $\mathcal{N}_2$ , on a line with configuration 722 and length

of 3840 feet. A second open switch was placed between node 1725 of  $\mathcal{N}_1$  and node 2725 of  $\mathcal{N}_2$ , on a line with configuration 722 and length of 3840 feet.

Four quadrant capable DER were placed on all existing phases at nodes  $\mathcal{G}_1 = \{1702, 1704, 1724, 1729, 1732, 1735, 1737, 1711\}$  and  $\mathcal{G}_2 = \{2702, 2704, 2724, 2729, 2735, 2737, 2711\}$ , with  $\mathcal{G} = \mathcal{G}_1 \cup \mathcal{G}_2$ . We assumed each DER can inject or sink both active and reactive power separately on each phase of the feeder and are only constrained by an apparent power capacity limit on each phase of 0.05 p.u., such that  $\bar{w}_n^\phi = 0.05, \forall \phi \in \mathcal{P}_n, \forall n \in \mathcal{G}$  and  $w_n^\phi = \bar{w}_n^\phi = 0 \forall \phi \in \mathcal{P}_n, \forall n \notin \mathcal{G}$ .

In this experiment, our objective was to close the two open switches sequentially, so as to connect  $\mathcal{T}_1$  and  $\mathcal{T}_2$  on two tie lines. We designed the OPF (23) to manage DER in for this purpose. Our experiment consisted of four steps. First, DER was dispatched according to (23), with  $k_1 = 1731$  and  $k_2 = 2731$  to minimize the phasor difference between nodes 1731 and 2731. Second, the switch between nodes 1731 and 2731 was closed, forming line (1731, 2731), such that  $\mathcal{E} \leftarrow \mathcal{E} \cup (1731, 2731)$ . Third, DER was dispatched according to (23), with  $k_1 = 1725$  and  $k_2 = 2725$  to minimize the phasor difference between nodes 1725 and 2725. Fourth, the switch between nodes 1725 and 2725 was closed, forming line (1725, 2725), such that  $\mathcal{E} \leftarrow \mathcal{E} \cup (1725, 2725)$ . The reader should note that after the first switch is closed, the aggregate network is no longer radial, and SDP approaches may have difficulty in optimizing this meshed network [9].

$$\begin{aligned}
& \underset{u_n^\phi, v_n^\phi, E_n^\phi, \theta_n^\phi, P_{mn}^\phi, Q_{mn}^\phi}{\text{minimize}} & & \rho_E C_E + \rho_\theta C_\theta + \rho_w C_w \\
& \text{subject to} & & (15) - (22), \\
& & & \underline{E} \leq E_n^\phi \leq \bar{E} \quad \forall \phi \in \mathcal{P}_n, \forall n \in \mathcal{N}, \\
& & & \mathbf{E}_\infty = [1, 1, 1]^T, \\
& & & \boldsymbol{\theta}_\infty = [0, -2\pi/3, 2\pi/3]^T, \\
& & & |w_n^\phi| \leq \bar{w}_n^\phi \quad \forall \phi \in \mathcal{P}_n, \forall n \in \mathcal{G}, \\
& & & C_E = \sum_{\phi \in \mathcal{P}_{k_1, k_2}} (E_{k_1}^\phi - E_{k_2}^\phi)^2, \\
& & & C_\theta = \sum_{\phi \in \mathcal{P}_{k_1, k_2}} (\theta_{k_1}^\phi - \theta_{k_2}^\phi)^2, \\
& & & C_w = \sum_{n \in \mathcal{G}} \sum_{\phi \in \mathcal{P}_n} |w_n^\phi|^2.
\end{aligned} \tag{23}$$

For both switching actions, we consider two cases. In the “No Control” (NC) Case, all DER dispatch is 0. In the “Phasor Control” (PC) Case for the both switching actions, the optimal DER dispatch is given by (23) with  $\rho_E = 1000$ ,  $\rho_\theta = 1000$ , and  $\rho_w = 1$ .

Table I clearly shows the voltage phasor difference between nodes 1731 and 2731 is minimized in both switching actions. Table I also demonstrates that the power flow across the closed switch (steady state power flow across the line with DER dispatch from (23)) is orders of magnitude smaller than the NC case.

**TABLE I: SIMULATION RESULTS FOR FIRST AND SECOND SWITCHING ACTIONS.**

	Phase $\phi$	First Switching Action $k_1 = 1731, k_2 = 2731$		Second Switching Action $k_1 = 1725, k_2 = 2725$	
		No Control	Phasor Control	No Control	Phasor Control
Node $k_1$ Voltage Phasor [p.u.] $V_{k_1}^\phi$	$a$	$0.9784 \angle -0.5147^\circ$	$0.9765 \angle -0.5587^\circ$	$0.9882 \angle -0.3003^\circ$	$0.9872 \angle -0.3257^\circ$
	$b$	$0.9909 \angle -120.3949^\circ$	$0.9901 \angle -120.4279^\circ$	$0.9882 \angle -120.2812^\circ$	$0.9833 \angle -120.3048^\circ$
	$c$	$0.9749 \angle 119.4164^\circ$	$0.9727 \angle 119.3669^\circ$	$0.9882 \angle 119.3006^\circ$	$0.9787 \angle 119.2415^\circ$
Node $k_2$ Voltage Phasor [p.u.] $V_{k_2}^\phi$	$a$	$0.9747 \angle -0.6021^\circ$	$0.9765 \angle -0.5580^\circ$	$0.9861 \angle -0.3508^\circ$	$0.9871 \angle -0.3255^\circ$
	$b$	$0.9893 \angle -120.4620^\circ$	$0.9901 \angle -120.4290^\circ$	$0.9861 \angle -120.3289^\circ$	$0.9832 \angle -120.3052^\circ$
	$c$	$0.9706 \angle 119.3172^\circ$	$0.9727 \angle 119.3669^\circ$	$0.9861 \angle 119.1815^\circ$	$0.9786 \angle 119.2407^\circ$
Voltage Magnitude Difference [p.u.] $ V_{k_1}^\phi  -  V_{k_2}^\phi $	$a$	0.0037	0.0000	0.0020	0.0001
	$b$	0.0015	0.0000	0.0026	0.0000
	$c$	0.0043	0.0000	0.0033	0.0000
Voltage Angle Difference [°] $\theta_{k_1}^\phi - \theta_{k_2}^\phi$	$a$	0.0874	-0.0007	0.0505	-0.0002
	$b$	0.0671	0.0011	0.0477	0.0004
	$c$	0.0991	-0.0000	0.1190	0.0009
Steady State Line Power Power [p.u.] $S_{k_1, k_2}^\phi$	$a$	$0.0852 + j0.0348$	$0.0005 + j0.0005$	$0.0581 + j0.0252$	$0.0013 + j0.0011$
	$b$	$0.0673 + j0.0221$	$0.0010 + j0.0004$	$0.0808 + j0.0316$	$0.0008 + j0.0008$
	$c$	$0.1100 + j0.0442$	$0.0001 + j0.0005$	$0.0867 + j0.0280$	$0.0009 + j0.0006$

#### IV. CONCLUSION

In this work, we extended a linear model of unbalanced distribution power flow to include a linear mapping between complex power flow on a line, and the voltage phasor angle at each end of the line. This extended model allows the formulation of OPF problems that manage the entire voltage phasor, rather than only voltage magnitude. The model is designed to be incorporated into convex optimal power flow problems, with the intention of enabling better switching in distribution networks. The complete linear model is presented in Section II-E.

In Section III, we formulated an OPF to manage DER to minimize the voltage phasor difference across an open (or closed) switch. Simulation results demonstrate the effectiveness of the OPF in minimizing voltage phasor difference between two disconnected points in a radial and meshed network.

Future efforts in this area will include investigations into sequential quadratic programming (SQP) to improve model accuracy. Finally, we recognize that it may be difficult to solve a centralized OPF of this type in an on-line fashion due to lack of proper network models, real-time load information, and a robust communications system. Therefore, we have explored alternate approaches to solving centralized OPFs using model-free and low communication optimization techniques in our other works [15], [16], [17].

#### V. ACKNOWLEDGEMENTS

We would like to thank Werner van Westering and his colleagues at distribution utility Alliander, The Netherlands for insightful conversations and suggestions regarding the operation of network reconfiguration.

#### REFERENCES

- A. von Meier, E. Stewart *et al.*, “Precision Micro-Synchrophasors for Distribution Systems: A Summary of Applications,” *IEEE Transactions on Smart Grid*, vol. 8, no. 6, pp. 2926–2936, Nov. 2017.
- “Synchrophasor fact sheet,” accessed, June-2010. [Online]. Available: [https://cdn.selinc.com/assets/Literature/Product%20Literature/Flyers/FS\\_Synchrophasor\\_BF\\_20100617.pdf?v=20150408-131001](https://cdn.selinc.com/assets/Literature/Product%20Literature/Flyers/FS_Synchrophasor_BF_20100617.pdf?v=20150408-131001)
- L. F. Ochoa and D. H. Wilson, “Angle constraint active management of distribution networks with wind power,” in *Innovative Smart Grid Tech. Conf. Europe (ISGT Europe)*. IEEE, Oct. 2010, pp. 1–5.
- D. Wang, D. Wilson *et al.*, “PMU-based angle constraint active management on 33kV distribution network,” in *22nd Int. Conf. Elect. Distribution*. IET, 2013, pp. 1–4.
- “Grid modernization multi-year program plan,” accessed Aug.-2015. [Online]. Available: <http://energy.gov/sites/prod/files/2016/01/f28/Grid%20Modernization%20Multi-Year%20Program%20Plan.pdf>
- “Quadrennial energy review: First installment,” accessed Apr.-2015. [Online]. Available: <http://energy.gov/epsa/downloads/quadrennial-energy-review-first-installment>
- É. Dall’Anese, H. Zhu, and G. Giannakis, “Distributed optimal power flow for smart microgrids,” *IEEE Trans. Smart Grid*, vol. 4, no. 3, pp. 1464–1475, Sept. 2013.
- B. C. Lesieutre, D. K. Molzahn *et al.*, “Examining the limits of the application of semidefinite programming to power flow problems,” in *Communication, Control, and Computing (Allerton), 2011 49th Annual Allerton Conference on*. IEEE, 2011, pp. 1492–1499.
- R. Madani, S. Sojoudi, and J. Lavaei, “Convex relaxation for optimal power flow problem: Mesh networks,” *IEEE Trans. Power Syst.*, vol. 30, no. 1, pp. 199–211, Jan. 2015.
- M. D. Sankur, “Optimal control of commercial office battery systems, and grid integrated energy resources on distribution networks,” Ph.D. dissertation, UC Berkeley, 2017.
- L. Gan and S. H. Low, “Convex relaxations and linear approximation for optimal power flow in multiphase radial networks,” in *2014 Power Syst. Computation Conf. (PSCC)*. IEEE, Aug. 2014, pp. 1–9.
- B. A. Robbins and A. D. Domínguez-García, “Optimal reactive power dispatch for voltage regulation in unbalanced distribution systems,” *IEEE Trans. Power Syst.*, vol. 31, no. 4, pp. 2903–2913, July 2016.
- D. B. Arnold, M. D. Sankur *et al.*, “Optimal dispatch of reactive power for voltage regulation and balancing in unbalanced distribution systems,” in *2016 IEEE Power Energy Soc. Gen. Meeting (PESGM)*, July 2016, pp. 1–5.
- “IEEE distribution test feeders,” accessed May-2015. [Online]. Available: <http://ewh.ieee.org/soc/pes/dsacom/testfeeders/index.html>
- D. B. Arnold, M. D. Sankur *et al.*, “Model-free optimal coordination of distributed energy resources for provisioning transmission-level services,” *IEEE Trans. Power Syst.*, vol. 33, no. 1, pp. 817–829, Jan. 2018.
- M. D. Sankur and D. Arnold, “Extremum seeking control of distributed energy resources with decaying dither and equilibrium-based switching,” in *Proceedings of the 52nd Hawaii International Conference on System Sciences*, 2019.
- M. D. Sankur, R. Dobbe *et al.*, “Model-free optimal voltage phasor regulation in unbalanced distribution systems,” *IEEE Transactions on Smart Grid*, vol. 11, no. 1, pp. 884–894, 2019.